BCSJ Award Article

Phase Separation of Phosphatidylcholine–Water Systems below the Main Transition Temperature Induced by Monovalent Ions

Kazuhiro Fukada*[1] and Nobuhiro Miki[2]

[1]Department of Applied Biological Science, Faculty of Agriculture, Kagawa University, 2393 Ikenobe, Miki-cho, Kagawa 761-0795

[2]Department of Chemistry, Graduate School of Science, Tokyo Metropolitan University, 1-1 Minami-Osawa, Hachioji, Tokyo 192-0397

Received October 7, 2008; E-mail: fukada@ag.kagawa-u.ac.jp

Effects of 1:1 electrolytes (LiCl, NaCl, NaBr, KCl, RbCl, and NH_4Cl) on the stacked multilamellar structure of phosphatidylcholine–water systems below the acyl-chain melting temperature were examined by means of small-angle X-ray scattering and differential scanning calorimetry. For the ternary DPPC–salt–water system at 20 °C, the lamellar repeating distance, D, jumped from 64 to 72 Å at certain thresholds of electrolyte concentration; 4.0, 2.1, and 1.4 mol kg^{-1} when LiCl, NaCl, or KCl were added, respectively. The temperature-dependent D jump from 72 to 64 Å at 20 °C was also confirmed for DPPC in 2.1 mol kg^{-1} NaCl accompanying the small latent heat of ca. 0.033 J g^{-1}. For the DMPC–NaCl–water system at 5 °C, the salt-induced D jump, at a threshold NaCl concentration of 1.2 mol kg^{-1}, was also observed. A triangular phase diagram of DPPC–NaCl–water at 20 °C was constructed based on X-ray scattering data. It was confirmed that the DPPC–NaCl–water system had a three-phase coexisting region, i.e., two lamellar phases with different repeating distances of 64 or 72 Å, respectively, and the NaCl bulk solution. Some qualitative aspects are discussed concerning the interpretation of the phase separation into the two different lamellar phases based on the lipid–monovalent ion interactions.

A multilamellar structure of lipid bilayer membranes in aqueous media is an optimal model system for exploring the forces acting between stacked plates. With respect to the important interactions between lipid membranes, van der Waals, electrostatic, hydration, and undulation forces have been considered.[1,2] These inter-bilayer forces compete with one another, and the net balance between attractive and repulsive forces control the equilibrium bilayer–bilayer separation, i.e., water layer thickness, D_w, of the multilamellar lipid bilayer systems. If we change the physicochemical properties of the lipid or medium materials, the force balance should also change and D_w will increase or decrease depending on the direction of the force balance shift. In other words, one can regard the inter-bilayer distance as an indicator of the force balance between the lipid membranes.

So far, we have explored the factors that can affect the inter-bilayer distance of phosphatidylcholines (PCs) above their main transition temperature, T_m, where acyl chains of PC molecules melt and the repulsive undulation force is significant. We have found that the lamellar repeating distance, D, for PCs decreased when D_2O was used as the dispersion medium instead of H_2O, which suggested the possibility of lowered contribution of undulation force in D_2O than in H_2O.[3] Conversely, the inter-bilayer distance for dimyristoylphosphatidylcholine multilamellar increased when gramicidin A (a hydrophobic peptide with no electric charge) was incorporated into the bilayer membranes.[4] This result suggested that the bending elasticity of membranes decreased by incorporating gramicidin A, leading to an increase of repulsive undulation force.

When electrically neutral PCs are used as the bilayer-forming material at a temperature below T_m, where PCs are in a solid-like gel phase ($L_{\beta'}$), one can rule out both the long-range electrostatic and undulation forces from the inter-bilayer interactions. In this situation, the force balance between the attractive van der Waals and repulsive hydration force would control the equilibrium inter-bilayer distance. Although biologically relevant lipids are usually in a fluid-like phase (L_α), studies on $L_{\beta'}$ phase are still valuable as a stepping-stone for understanding the structure and interactions of lipid bilayers.[5] This study examines how monovalent ions affect the inter-bilayer distance of gel-state PCs where the inter-bilayer separation is within a few nanometers and how they can change phase behaviors of hydrated PC systems.

Published on the web April 11, 2009; doi:10.1246/bcsj.82.439

Experimental

Materials. Freeze-dried powder of 1,2-dipalmitoyl-*sn*-glycero-3-phosphocholine (DPPC), 1,2-dimyristoyl-*sn*-glycero-3-phosphocholine (DMPC), and 1,2-dilauroyl-*sn*-glycero-3-phosphocholine (DLPC) was purchased from Avanti Polar Lipids (Birmingham, AL). We confirmed by phosphorus content analysis that the DPPC, DMPC, and DLPC samples used in this study contained 1.0, 2.0, and 1.4 water molecules per lipid molecule, respectively. These lipid samples were used without further purification. Guaranteed grade LiCl, KCl, RbCl, NH_4Cl, and NaBr were purchased from Wako Chemicals (Osaka, Japan) and NaCl from Matsunaga Chemical (Fukuyama, Japan). Water was purified by passing it through a Milli-Q Labo system (Millipore, Bedford, MA) after distillation.

Sample Preparation. Prescribed amounts of lipid powder were weighed out in a screw-top V-shaped glass vial (Wheaton, Millville, NJ), and swollen by the addition of an aqueous salt solution containing 10 μM ($1\,M = 1\,mol\,dm^{-3}$) NaN_3 as an antiseptic. The lipid–salt–water mixtures were then annealed by more than ten cycles of cooling at 0 °C and heating at 52 °C, and were aged for 1–2 days at room temperature. These samples were used for small-angle X-ray scattering (SAXS) and differential scanning calorimetry (DSC). The lipid concentrations were ca. 20–85 wt % for SAXS and ca. 35 wt % for DSC.

Small-Angle X-ray Scattering. Small-angle X-ray scattering (SAXS) was measured using a high-resolution small-angle X-ray scattering instrument (Mac Science Co., Tokyo) equipped with a tungsten/silicon multilayer monochromator. Monochromatic Cu Kα radiation ($\lambda = 0.154$ nm) from a rotating anode (SRAMXP18) working at 40 kV and 350 mA was focused by a Kratky slit and introduced to the samples. A digital imaging plate (DIP200) detected the scattered X-ray. The length from the sample to the detector was ca. 1.09 m. The lipid–salt–water mixture was placed in a 1-mm thick Mylar-film-window cell, and the thermostat cell holder was regulated to ±0.1 °C. Lamellar repeat distance, D, was calculated from the peak position of the diffracted X-rays using the Bragg equation; $D = 2\pi n/q$, where n is an integer and $q = 4\pi \sin\theta/\lambda$ (2θ is the scattering angle).

Construction of Triangular Phase Diagram. A triangular ternary phase diagram of the DPPC–NaCl–water system was constructed based on the variation of SAXS patterns observed with the change of gross composition. In the binary DPPC–water system, the SAXS peak positions did not change with composition as long as the system contained two phases ($L_{\beta'}$ + bulk water). Below a threshold water content, however, the peak positions shifted gradually toward higher scattering angles with lipid content because of the absence of bulk water phase and the decrease of inter-lamellar spacing, suggesting that the system was one phase ($L_{\beta'}$). The same phase behavior was true for the DPPC–NaCl–water system if the NaCl content was rather low. Above a threshold of NaCl content where diffraction different from $L_{\beta'}$ was observed, the system was in a two-phase state containing the NaCl solution and a different type of lamellar phase from $L_{\beta'}$. If two separate diffractions (one of which was $L_{\beta'}$) were observed simultaneously, the system consisted of three phases (two types of lamellar phase + NaCl solution). By knowing the phase state at various gross compositions for DPPC–NaCl–water at 20 °C, the phase boundaries were determined to give the triangular phase diagram.

Differential Scanning Calorimetry. Differential scanning calorimetry (DSC) was performed with a Micro-DSC VII system (Setaram S. A., France) at a heating rate of $0.2\,K\,min^{-1}$. The prepared lipid–salt–water mixture (ca. 230 mg) was put in a closed Hastelloy vessel. Aqueous NaCl was used as the reference.

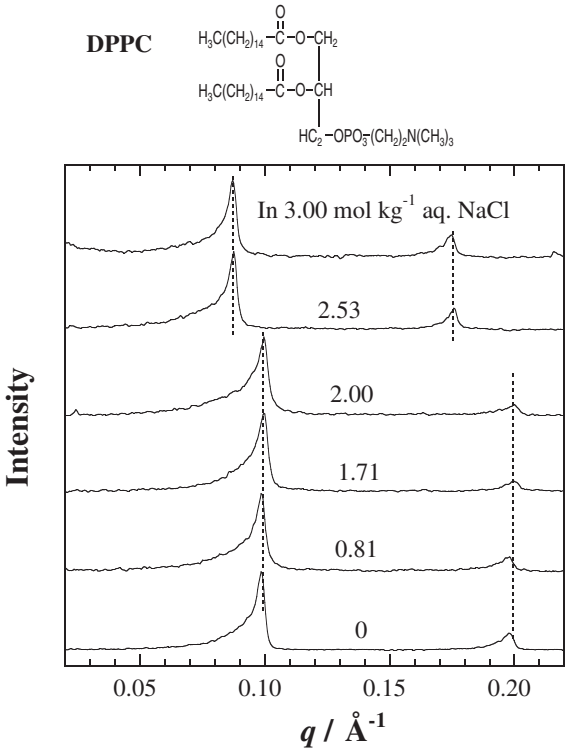

Figure 1. Representative small-angle X-ray diffraction patterns from fully hydrated DPPC dispersed in aqueous NaCl solution at 20 °C. Concentration of NaCl is indicated in molality units. Content of DPPC was ca. 35 wt %. q is magnitude of scattering vector: $q = 4\pi \sin\theta/\lambda$, where 2θ is scattering angle and λ is the wavelength of incident X-ray. Vertical broken lines have been added to show the peak-top shift.

Results

Change of SAXS Patterns with Salt Concentration. Figure 1 shows the small-angle X-ray diffraction patterns for DPPC dispersed in NaCl aqueous solution with various concentrations at 20 °C. It is well known that hydrated DPPC at 20 °C is in an $L_{\beta'}$ state and one can clearly observe the Bragg reflections from the stacked multilamellar structure. We can see in Figure 1 that two diffraction peaks corresponding to the first and second reflections by the stacked lamellar structure were detected for each sample. The peak-top position of the first (and second) peak shifted from $0.098\,Å^{-1}$ ($0.198\,Å^{-1}$) to $0.089\,Å^{-1}$ ($0.173\,Å^{-1}$) when the concentration of NaCl in dispersion medium increased from 2.00 to 2.53 mol kg^{-1}. When performing SAXS measurements for DPPC, not only in NaCl solution but also in other monovalent salt solutions, the same sort of X-ray diffraction patterns were obtained. The lamellar repeating distance, D, was calculated using the Bragg equation and plotted against the electrolyte concentration in Figure 2. All 1:1 electrolytes studied induced the D jump from ca. 64 to ca. 72 Å at some threshold concentration. It is interesting to note that RbCl is the most effective for the D jump, versus LiCl, which is the least effective, and the threshold concentrations are

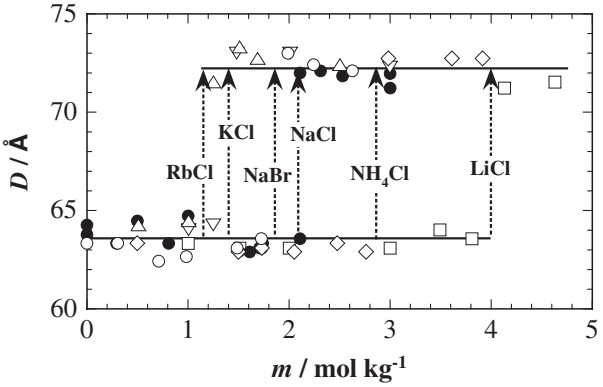

Figure 2. Lamellar repeating distance of the multilamellar phase of DPPC, *D*, dispersed in aqueous 1:1 electrolyte solutions as a function of the electrolyte concentration. Temperature was 20 °C. Content of DPPC was ca. 35 wt % where DPPC was fully hydrated. Different symbols represent the different electrolytes; ●: NaCl, ○: NaBr, □: LiCl, ▽: KCl, △: RbCl, and ◇: NH_4Cl. Arrows indicate the salt concentrations where the *D* jump occurred.

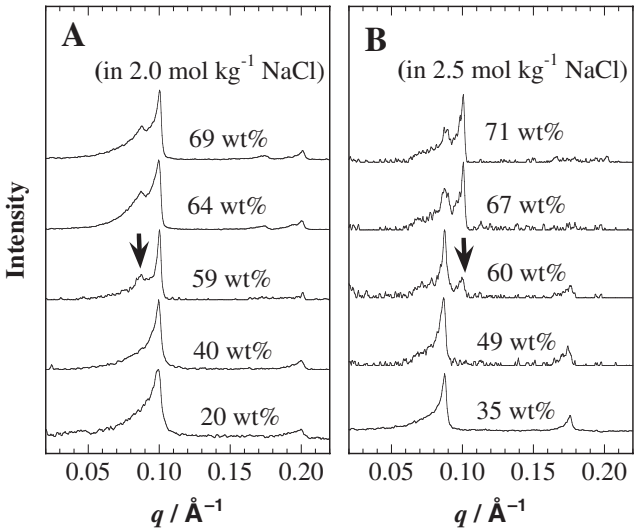

Figure 3. Small-angle X-ray diffraction patterns from hydrated DPPC dispersed in 2.0 mol kg^{-1} aqueous NaCl (A) and 2.5 mol kg^{-1} aqueous NaCl (B). Temperature was 20 °C. Content of DPPC in each sample is indicated in the figure. Arrows point to the newly emerged diffraction accompanying increasing DPPC content.

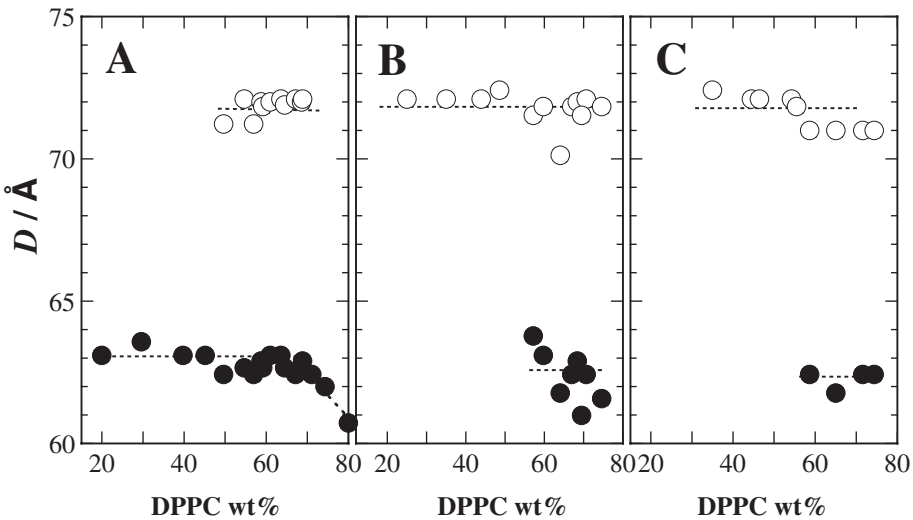

Figure 4. Lamellar repeating distance of the multilamellar phase of DPPC, *D*, dispersed in aqueous NaCl solutions as a function of DPPC content in the system. Temperature was 20 °C. Concentrations of the NaCl solution were 2.0 (A), 2.5 (B), and 3.0 mol kg^{-1} (C), respectively. Open and closed symbols correspond to the X-ray diffraction of $q \approx 0.089$ and 0.098 $Å^{-1}$, respectively.

according to the Hofmeister series for anions ($Cl^- > Br^-$) and cations ($Li^+ > Na^+ > K^+ > Rb^+$) except in NH_4^+.

Rappolt et al. reported the effects of alkali-metal chlorides (LiCl, NaCl, and KCl) on PC–water bilayer systems in the L_α phase by means of SAXS.[6,7] They had observed splitting of the X-ray diffraction peaks induced by alkali chlorides for distearoyl, palmitoyl–oleyl, and egg phosphatidylcholine multilamellar bilayer. Their results suggested the formation of discretely different multilamellar lattices by the addition of 1:1 electrolytes, and three Lorentz distributions fit the SAXS peaks, assuming three different lamellar phases coexisted.[6] On the other hand, for DLPC multilayer in KCl and KBr solutions at 15, 25, and 35 °C where DLPC is in the L_α-state, a gradual increase of *D* was confirmed with increasing salt concentration.[8]

Change of SAXS Patterns with Lipid Content. During the next step, we focused on the DPPC–NaCl–water system and closely examined the dependence of SAXS patterns on lipid content. Figure 3 shows the typical example for SAXS patterns of DPPC dispersed in 2.0 and 2.5 mol kg^{-1} NaCl as a function of DPPC weight fraction in the system. When the lipid content was below 50 wt %, the peak-top position of the first diffraction was 0.098 $Å^{-1}$ (0.089 $Å^{-1}$) in 2.0 (2.5) mol kg^{-1} NaCl. By increasing the lipid content up to ca. 60 wt %, a new X-ray diffraction peak emerged, indicated by the thick arrows in Figure 3. Since two different diffraction peaks were simulta-

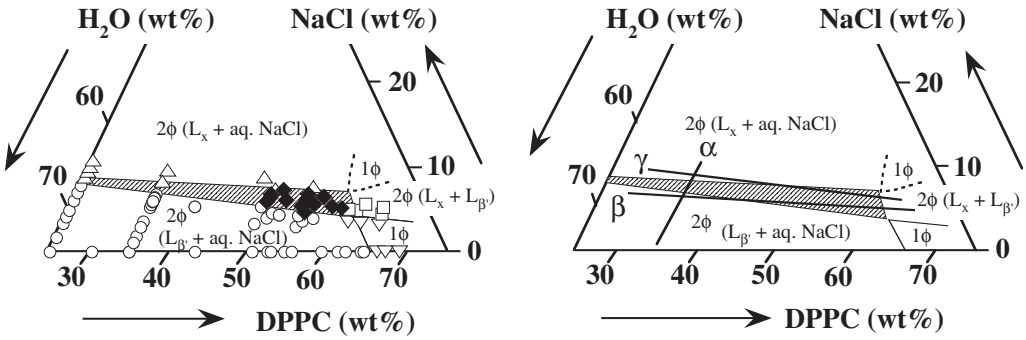

Figure 5. Triangular phase diagram for the DPPC–NaCl–water system at 20 °C. 1ϕ and 2ϕ represent one-phase and two-phase coexisting regions, respectively. The shaded area indicates the three-phase coexisting composition region. Left panel: Plots represent the composition at which SAXS were performed in this study. Different symbols represent the different lamellar repeating distances, D, observed by SAXS; $D = 64$ Å (○), $D < 64$ Å (▽), $D = 72$ Å (△), $D < 64$ Å and $D < 72$ Å (□), and $D = 64$ and 72 Å (◆). Right panel: The changes of sample composition for SAXS in Figures 1, 3A, and 3B are indicated by lines α, β, and γ, respectively.

neously detected, two types of lamellar phases coexisted in these samples.

Based on these SAXS measurements, the lamellar repeating distance of DPPC in aqueous NaCl was plotted against lipid content in Figure 4. Both Figure 2 and Figure 4 suggested that the possible lamellar repeating distances for fully hydrated DPPC at 20 °C were only 64 or 72 Å, and it seems reasonable to consider the D jump as an indication of phase separation. Thus, a triangular phase diagram for DPPC–NaCl–water system was constructed as described below.

Triangular Phase Diagram of DPPC–NaCl–Water System. The best way to show how phase equilibriums vary with composition in a ternary system is to use a triangular phase diagram.[9,10] For the DPPC–NaCl–water system at 20 °C, we have confirmed three phases to be considered; one bulk NaCl aqueous solution and two lamellar phases with different lamellar repeating distances of 64 ($L_{\beta'}$) and 72 Å (tentatively named as L_x). Considering the phase boundary compositions suggested by Figures 1–4, we constructed the triangular phase diagram of the DPPC–NaCl–water ternary system in Figure 5.

The most interesting feature of the DPPC–NaCl–water phase diagram is the presence of the three-phase coexisting region (shaded area in Figure 5). Here, let us consider what would happen if the NaCl content increases from 0 to 10 wt % at a constant DPPC weight fraction of 35 wt %. In this situation, the composition of the system moves from the lower 2ϕ (NaCl aqueous solution + $L_{\beta'}$) to the upper 2ϕ region (NaCl aqueous solution + L_x) along line α crossing the narrow three-phase region (see the right panel of Figure 5). One should therefore observe the D jump from 64 to 72 Å as shown in Figure 2. On the contrary, if we successively add DPPC into 2.0 mol kg^{-1} (3.0 mol kg^{-1}) NaCl aqueous solution, the gross composition will change along line β (line γ) in Figure 5. When the gross composition enters the three-phase region (NaCl aqueous solution + $L_{\beta'}$ + L_x), splitting of SAXS diffraction should be observed as Figure 3. In this way, Figure 5 can explain all the SAXS patterns observed for the DPPC–NaCl–water system at 20 °C accompanying the gross composition change.

Temperature Stability of L_x State. It is interesting to examine the temperature stability of the newly found L_x-phase

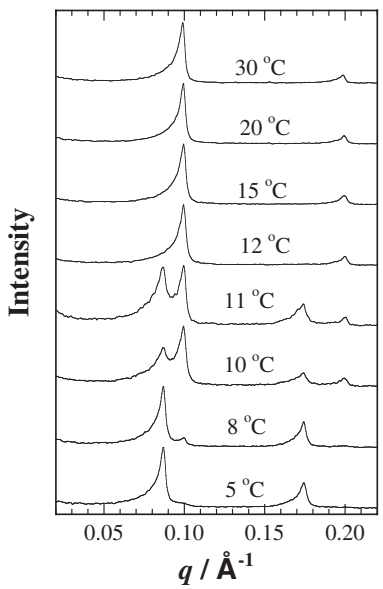

Figure 6. Small-angle X-ray diffraction patterns from fully hydrated DPPC dispersed in 1.7 mol kg^{-1} NaCl aqueous solutions at various temperatures. Content of DPPC was ca. 35% by weight.

for the DPPC–NaCl–water system. We performed SAXS measurements for 35 wt % DPPC dispersed in 1.7 mol kg^{-1} NaCl at various temperatures which formed $L_{\beta'}$ at 20 °C. Figure 6 shows the diffraction at 0.098 Å^{-1} from $L_{\beta'}$ between 12 and 30 °C. On reducing the temperature to 11 °C, the diffraction at 0.089 Å^{-1} from L_x-phase emerges, and both $L_{\beta'}$ and L_x coexist between 8 and 11 °C. At 5 °C, the transition from $L_{\beta'}$ to L_x is complete and the diffraction from L_x remains. We further performed the SAXS measurements for hydrated DPPC in different concentrations of aqueous NaCl, and the lamellar repeating distance was plotted as a function of temperature in Figure 7. It can be seen in Figure 7 that hydrated DPPC only forms $L_{\beta'}$ in pure water and no D jump is observed in the temperature range studied. In 1.7 and 2.1 mol kg^{-1} NaCl, however, the D jump from 64 to 72 Å occurs at around 10 and 20 °C, respectively. Figure 7 clearly suggests

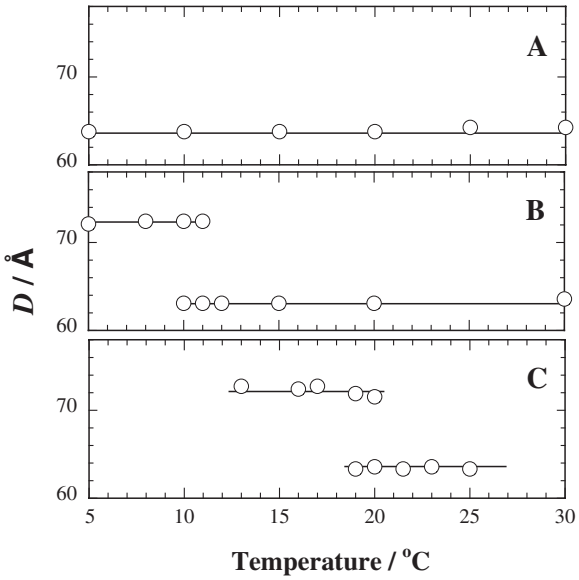

Figure 7. Temperature dependence of lamellar repeating distance of multilamellar phase, D, for DPPC dispersed in aqueous NaCl solution. Content of DPPC was ca. 35 wt %. Concentrations of NaCl solution were 0 (A), 1.70 (B), and 2.11 mol kg^{-1} (C), respectively.

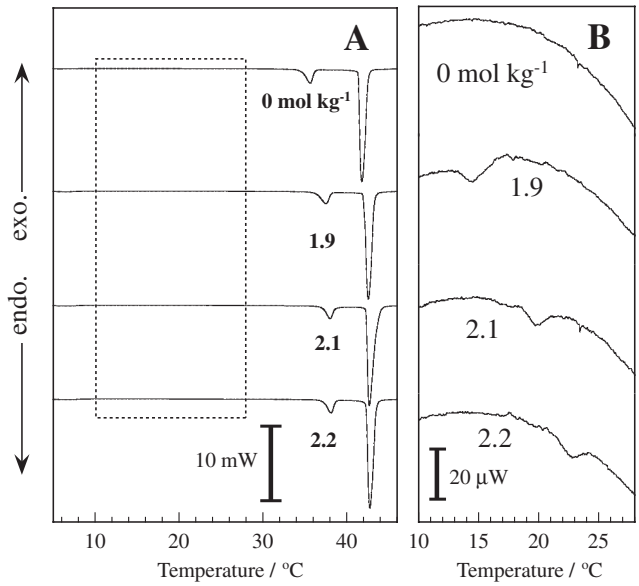

Figure 8. DSC heating thermograms for fully hydrated DPPC in aqueous NaCl solutions. Concentration of the NaCl solution is indicated in molality units. (A) indicates the original DSC curves, and the broken-lined box region is redrawn in (B) with 350-fold magnification of the vertical scale.

Table 1. Temperature (T) and Enthalpy Change (ΔH) for Transitions of DPPC in Various Aqueous NaCl Solutions Detected by DSC

NaCl concentration /mol kg^{-1}	L_x–$L_{\beta'}$		Pre transition ($L_{\beta'}$–$P_{\beta'}$)		Main transition ($P_{\beta'}$–L_α)	
	T/°C	ΔH/J g^{-1}	T/°C	ΔH/J g^{-1}	T/°C	ΔH/J g^{-1}
0	—	—	34.6	7.4	41.4	45.2
1.9	14.5[a)]	0.052	36.3	6.7	42.0	44.2
2.1	19.7[a)]	0.033	37.2	5.7	42.3	43.5
2.2	22.7[a)]	0.027	37.2	6.5	42.3	43.3

a) Peak-top temperature for the DSC curve in Figure 8B.

that the formation of L_x is more favorable than $L_{\beta'}$ in higher concentration NaCl solutions and at lower temperatures.

Considering the temperature-induced D jump in Figure 7, we expect that temperature-scanning calorimetric methods might provide valuable information for the L_x–$L_{\beta'}$ transition, and performed DSC measurements (Figure 8). We can confirm that both the pre-transition (ca. 35 °C) and main-transition (ca. 42 °C) of fully hydrated DPPC increases slightly with NaCl concentration, as has been reported,[11] and a small but noticeable endothermic peak is detected accompanying the L_x–$L_{\beta'}$ transition which occurred around 15, 20, and 23 °C in 1.9, 2.1, and 2.2 mol kg^{-1} NaCl, respectively (Figure 8B). Thermodynamic quantities for the transitions are summarized in Table 1.

Effects of Acyl-Chain Length of Lipid. Finally, we tried to see the effect of the acyl-chain length of lipids on the $L_{\beta'}$–L_x transition in aqueous NaCl. We measured the lamellar repeating distance for DMPC at 5 °C, DLPC at 20 °C, and DPPC at 5, 20, 30, and 50 °C as a function of NaCl concentration (Figure 9). It should be noted that DMPC (and DPPC) at 5 °C (5, 20, and 30 °C) is $L_{\beta'}$ whereas DLPC at 20 °C and DPPC at 50 °C are in L_α phase, respectively. At 5 °C, one can see that a D jump of DMPC from 63 to 71 Å occurred at 1.2 mol kg^{-1} NaCl whereas a D jump from 64 to 72 Å occurred for DPPC at 1.6 mol kg^{-1} NaCl. For PCs in L_α phase on the other hand, only the gradual increase of D with NaCl concentration was confirmed. Figure 9 also shows that below the main-transition temperature of DPPC, the D jump occurred at the lower NaCl concentration when the temperature was lowered. These results suggested the increased stability of L_x-phase at lower temperatures.

Discussion

For a DPPC–NaCl–water ternary system at 20 °C, the change of lamellar repeating distance, D, with gross composition could be well demonstrated by a triangular phase diagram (Figure 5). In the phase diagram, there were two types of lamellar phases; $L_{\beta'}$ ($D = 64$ Å) and L_x ($D = 72$ Å). The same may be true for the phase behavior of DPPC in other 1:1 electrolyte solutions at 20 °C as well as for DMPC–NaCl–water at 5 °C. Further, DSC measurements confirmed that the thermal L_x–$L_{\beta'}$ transition occurred with very little latent heat. The features of L_x state are as follows: 1) L_x becomes more stable at lower temperature

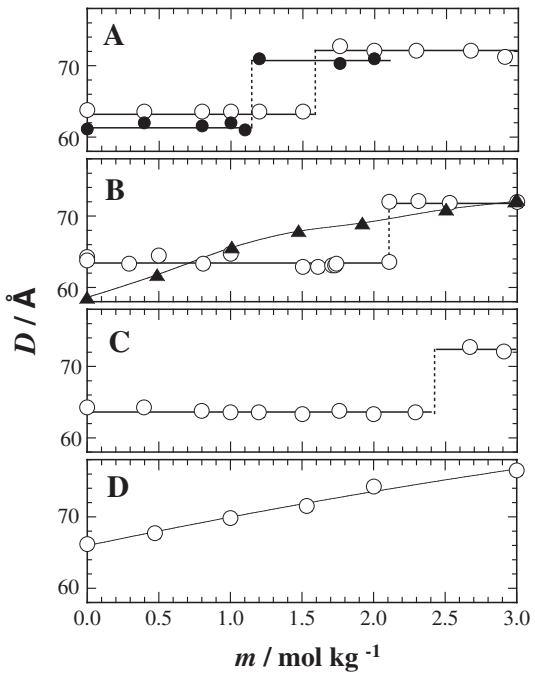

Figure 9. Lamellar repeating distance of multilamellar phase, *D*, of DPPC (○), DMPC (●), and DLPC (▲) dispersed in aqueous NaCl solutions as a function of NaCl concentration at various temperatures. Temperatures were 5 (A), 20 (B), 30 (C), and 50 °C (D). Content of the lipid in each sample was ca. 35 wt %.

and in higher electrolyte concentration. 2) Enthalpy change for the thermal L_x–$L_{\beta'}$ transition is about a third-order smaller than that of the $P_{\beta'}$–L_α main-transition. 3) The lamellar repeating distance of L_x is ca. 8 Å larger than that of $L_{\beta'}$, which is close to the diameter of hydrated monovalent ions; 7.6 Å for Li^+, 7.2 Å for Na^+, 6.6 Å for K^+, and 6.6 Å for Cl^-.[12] At present, it is hard to explain these features with the lack of detailed structural information such as the electron density profile and acyl-chain packing state for L_x-phase. As such, we will limit our discussion here to some qualitative viewpoints which should be considered for the interpretation of $L_{\beta'}$–L_x transition, referring to some relating works by other researchers.

Thermal phase transitions of hydrated PCs have been closely studied through many different techniques, and thermodynamic quantities of transitions are well documented.[13] Three major transitions; sub-, pre-, and main-transition, are generally known to occur with the change of packing state of acyl-chains in a bilayer. On the other hand, the enthalpy for the L_x–$L_{\beta'}$ transition is extremely small, suggesting that the packing state of acyl-chains may not change so much during the transition. Instead of the packing state of acyl-chains, we hypothesize that the interacting state of monovalent ions with the PC bilayer is related to the L_x–$L_{\beta'}$ transition. Recent molecular dynamics simulations[14–16] and electrophoretic mobility measurements[17,18] have actually suggested that monovalent ions could bind to neutral PCs in salt solutions (<1 M). The accumulation of monovalent ions between lipid bilayers is presumed to be led by the attractive interaction of positive and negative ions to the zwitterionic PC bilayer surface.[19,20] A recent theoretical work based on a Monte Carlo simulation and correlation-corrected Poisson–Bolzmann theory successfully rationalized the lamellar–lamellar phase transition in surfactant bilayer systems by monovalent ion adsorption, although it predicted the sudden decrease of inter-lamellar spacing at a threshold salt concentration.[21]

The lamellar repeating distance is the sum of lipid bilayer thickness and inter-bilayer distance and it is not clear at the present stage how each of them changes during $L_{\beta'}$–L_x transition. To estimate the bilayer thickness and inter-bilayer distance, higher quality SAXS profiles are necessary. At any rate, if the binding of monovalent ions is the origin of $L_{\beta'}$–L_x transition, it seems natural to interpret the order of ions to the threshold concentration for *D* jump ($Cl^- > Br^-$ for anions and $Li^+ > Na^+ > K^+ > Rb^+$ for cations) as the order of affinity of ions to PC surface. This means that the lower the affinity, the higher the threshold concentration required to accumulate enough ions to induce the phase transition. Actually, it has been suggested through usage of a fluorescence technique that Br^- had a higher affinity to DMPC surface than Cl^-.[20] For monovalent cations that were much less efficient than anions however, Li^+ has the highest affinity in monovalent ions,[20] contrary to preceding expectations. This leads us to the idea that the binding of anions to PC surface is the main factor to induce L_x whereas cations suppress it, to be consistent with the presented results.

In relation to the PC–monovalent ion interaction, a study by Petrache et al. should be mentioned.[22] They observed that neutral PC multilamellar aggregates in L_α state sank in low KCl or KBr aqueous solutions at 20 °C, but floated in high salt solutions. Neutral buoyancy occurred in the salt solution that was much less dense than the lipid itself, suggesting salt exclusion from the inter-lamellar space of PC membranes. In our study however, the phase diagram for the DPPC–NaCl–water system (Figure 5) indicated that a lower NaCl content in the inter-lamellar space for $L_{\beta'}$ suggested exclusion, whereas a higher NaCl content for L_x suggested inclusion of NaCl. It is assumed that whether salt was excluded from or included into multilamellar aggregates depends on the subtle balances between lipid–water, ion–water, and lipid–ion interactions, which can significantly be influenced by the state of PC bilayer and environment conditions.

Finally, it is worthwhile to refer to the effects of divalent cations (Ca^{2+} and Mg^{2+}) on the lamellar repeating distance of fully hydrated DPPC in $L_{\beta'}$ state.[23] It has already been confirmed that the repeating distance jumped discontinuously from 64 Å to over 100–200 Å by adding small amounts of $CaCl_2$ or $MgCl_2$ (<10 mM), then decreased gradually with the salt concentration (10–200 mM), recovering the initial level of 64 Å in 200–1000 mM. These results, suggesting the strong affinity of divalent cations, were reasonably interpreted by taking into account three kinds of inter-bilayer interactions: electrostatic repulsion caused by adsorbed cation on the bilayer, van der Waals interaction, and repulsive interaction caused by hydration layers.[24,25] Compared to the effects of 1:1 electrolytes, which led to a negatively charged bilayer indicating preferential adsorption of anions than cations,[17,18] the effective concentration range for the *D* jump by 2:1 electrolytes was much lower than for 1:1 electrolytes. Concerning inter-bilayer interactions in L_x-phase, one can expect complete screening of

electrostatic repulsion because of the high salt concentration (>1 M). We suppose that an oscillatory steric-solvation force, which becomes significant when two rigid surfaces approach closer than a few nanometers,[26,27] may be playing an important role in the inter-bilayer interactions for the L_x-phase formation.

Conclusion

The phase behaviors of three-component PC–salt–water systems were investigated over a wide composition range by SAXS measurements and a triangular phase diagram was constructed for DPPC–NaCl–water system. When the system contained a large amount of NaCl (>2.1 mol kg^{-1} in aqueous phase), a new type of lamellar phase (tentatively named the L_x-phase) was found for the first time in this study. The lamellar repeating distance of L_x was ca. 8 Å larger than the $L_{\beta'}$ of DPPC. Interestingly, the salt-induced L_x-phase formation also occurred with the addition of another 1:1 electrolyte (LiCl, NaBr, KCl, RbCl, and NH_4Cl) to hydrated DPPC above a different threshold electrolyte concentration. When SAXS was measured at 5 °C for the DMPC–NaCl–water system, L_x-phase formation was confirmed at 1.2 mol kg^{-1} NaCl. Formation of L_x-phase by salt addition was only induced below the acyl-chain melting temperature of PCs. The temperature dependence of phase behavior for DPPC–NaCl–water was further examined, confirming that the L_x–$L_{\beta'}$ transition occurred during the heating process. Enthalpy change for L_x–$L_{\beta'}$ transition was three orders of magnitude smaller than that for $L_{\beta'}$–L_α main-transition. It was hypothesized that the binding of anions to the PC surface is the driving force for L_x-phase formation, whereas the binding of monovalent cations, which is much less efficient than anions, may suppress the L_x-phase formation. These results provide new insights into the effect of monovalent ions to bilayer structures and inter-bilayer interactions of zwitterionic PCs in salt solutions.

This work is financially supported by the Grant-in-Aid for Scientific Research by the Japan Society for the Promotion of Science (JSPS).

References

1 R. P. Rand, V. A. Parsegian, *Biochim. Biophys. Acta* **1989**, *988*, 351.
2 J. N. Israelachvili, *Intermolecular & Surface Forces*, 2nd ed., Academic Press, San Diego, **1991**, pp. 395–414.
3 Y. Kobayashi, K. Fukada, *Chem. Lett.* **1998**, 1105.
4 Y. Kobayashi, K. Fukada, *Biochim. Biophys. Acta* **1998**, *1371*, 363.
5 J. F. Nagle, S. Tristran-Nagle, *Biochim. Biophys. Acta* **2000**, *1469*, 159.
6 M. Rappolt, K. Pressl, G. Pabst, P. Laggner, *Biochim. Biophys. Acta* **1998**, *1372*, 389.
7 M. Rappolt, G. Pabst, H. Amenitsch, P. Laggner, *Colloids Surf., A* **2001**, *183–185*, 171.
8 H. Petrache, T. Zemb, L. Belloni, V. A. Parsegian, *Proc. Natl. Acad. Sci. U.S.A.* **2006**, *103*, 7982.
9 P. W. Atkins, in *Physical Chemistry*, 4th ed., ed. by W. H. Freeman, New York, **1990**, p. 199.
10 R. G. Laughlin, *The Aqueous Phase Behavior of Surfactants*, Academic Press, San Diego, **1994**, p. 368.
11 D. Chapman, W. E. Peel, B. Kingston, T. H. Lilley, *Biochim. Biophys. Acta* **1977**, *464*, 260.
12 J. N. Israelachvili, *Intermolecular & Surface Forces*, 2nd ed., Academic Press, San Diego, **1991**, p. 55.
13 D. M. Small, *The Physical Chemistry of Lipids* in *Handbook of Lipid Research*, Plenum Press, New York, **1986**, Vol. 4, pp. 485–486.
14 S. A. Pandit, D. Bostick, M. L. Berkowitz, *Biophys. J.* **2003**, *84*, 3743.
15 R. A. Böckmann, A. Hac, T. Heimburg, H. Grubmüller, *Biophys. J.* **2003**, *85*, 1647.
16 J. N. Sachs, H. Nanda, H. I. Petrache, T. B. Woolf, *Biophys. J.* **2004**, *86*, 3772.
17 S. A. Tatulian, *Biochim. Biophys. Acta* **1983**, *736*, 189.
18 J. Kotyńska, Z. A. Figaszewski, *Biochim. Biophys. Acta* **2005**, *1720*, 22.
19 H. Akutsu, J. Seelig, *Biochemistry* **1981**, *20*, 7366.
20 R. J. Clarke, C. Lüpfert, *Biophys. J.* **1999**, *76*, 2614.
21 J. Forsman, *Langmuir* **2006**, *22*, 2975.
22 H. I. Petrache, I. Kimchi, D. Harries, V. A. Parsegian, *J. Am. Chem. Soc.* **2005**, *127*, 11546.
23 Y. Inoko, T. Yamaguchi, K. Furuya, T. Mitsui, *Biochim. Biophys. Acta* **1975**, *413*, 24.
24 H. Ohshima, T. Mitsui, *J. Colloid Interface Sci.* **1978**, *63*, 525.
25 H. Oshima, Y. Inoko, T. Mitsui, *J. Colloid Interface Sci.* **1982**, *86*, 57.
26 J. N. Israelachvili, R. M. Pashley, *Nature* **1983**, *306*, 249.
27 J. N. Israelachvili, *Intermolecular & Surface Forces*, 2nd ed., Academic Press, San Diego, **1991**, pp. 260–287.